Optical and electrical properties of thin silver films grown under ion bombardment

F. Parmigiani,* E. Kay, T. C. Huang, J. Perrin, M. Jurich, and J. D. Swalen
IBM Almaden Research Center, San Jose, California 95120-6099
(Received 6 May 1985)

The structure of thin silver films, grown under varying conditions of ion bombardment, are compared by means of their measured structural, optical, and electrical properties. Both the x-ray diffraction results and the dielectric-function measurements suggested that there are voids in our films and that their volume fraction depends on the energy delivered to the substrate during growth. Furthermore, the same dependency on energy was found for the amount of gas atoms trapped in the films, but the low percentage suggests that this cannot have a major influence on the structure or other properties. However, the gas atoms can contribute to an expansion of the lattice by increasing the separation of the metallic grains and increasing the volume fraction of voids. The dc electrical conductivity was interpreted from the microstructure and optical data with a model including scattering at grain boundaries, the fraction of voids and the bulk conductivity. In particular, a comparison between theoretical and experimental data suggest that the electron reflection coefficient at the grain surfaces is not constant, but depends on the condition of film growth.

I. INTRODUCTION

The growth under ion bombardment of thin metal films has been a subject of great interest to those using physical vapor-deposition processes[1] because the structure and related physical properties can be modified and controlled as a function of the energy and ion flux delivered to a growing film.[2–12] We have shown[8–12] that two distinct regimes of ion bombardment exist: one regime, where the lattice parameters, the residual strain and the resistivity increase and the grain size decreases with increasing energy delivered to the substrate and another regime, which occurs at higher energies and higher deposition rate, where the reverse behavior is observed. In this work, only films belonging to the first regime will be considered.

Among the methods which use ion bombardment during film growth, radio frequency bias sputtering, triode sputtering, and ion plating are among the most common.[1] These methods, however, introduced uncertainties, some of which can be overcome by the use of dual ion beams: one to sputter the source material and the other to bombard the surface of the growing film on the substrate.[13–15]

The aim of this paper is to study the relationship of film structure to the optical and electrical properties of thin silver films, grown under ion bombardment, in a dual ion-beam UHV system. Although systematic studies of the optical properties of such films have not been reported, considerable theoretical and experimental work exists on the optical properties of noble metals deposited by conventional techniques.[16] Differences in the optical properties have been attributed to surface roughness, strain, grain-boundary effects, and voids.[17] Recently Aspnes[18] has analyzed the effects of voids on the optical properties of thin gold films. In the interband region, he shows that the imaginary part of the dielectric function depends strongly on the presence of voids, i.e., their volume fraction. In the free electron region, on the other hand, surface roughness and grain size can modify the imaginary part significantly, but the voids only change the imaginary part by the introduction of some additional scattering. The voids do decrease the magnitude of the real part because the plasma frequency depends on electron volume density.

We determined the dielectric function of our films by measuring the reflectivity minimum in an attenuated-total-reflection (ATR) configuration from a silver film at the base of a prism. Loss in reflectivity is caused by the surface plasmon absorption and the angular position, depth, and width of reflectivity versus angle of incidence, which can be fitted to the Fresnel reflectivity equations in order to determine the film thickness and the real and imaginary parts of the dielectric function. This ATR technique has been described elsewhere[19] and the reader is referred to this reference for more details.

A comparative analysis between our optical data and the measured strain, grain size, and lattice parameter suggests that the differences in dielectric function between the bulk metal and the ion-bombarded film arise mainly from the presence of voids and changes in grain size. The fraction of voids was determined from the dielectric function for a homogeneous sample of silver, our measured values of the dielectric function in the bombarded films, and the Bruggeman effective-media approximation (EMA). Independently, the void concentration was also calculated from the total amount of silver determined by x-ray fluorescence and the film thickness determined by ATR measurements. As expected, the void and grain-size values depend on the energy delivered to the film during its growth. A similar ion energy dependence was found for the amount of sputtering gas trapped in the films, though in all cases the amount was less than 1 at. %. We will present evidence showing that this small amount of gas cannot explain the observed structural changes, but the presence of voids could introduce a structural mismatch between the grains.

The analysis of the dc conductivity also takes into ac-

count the grain sizes and void fractions as derived from our optical and structural data. The electrical resistivity in the bulk material arises from the collision of the conduction electrons with the vibrating lattice atoms, defects, and impurities. To each of these processes can be attributed, at temperatures higher than the Debye's temperature, a characteristic relaxation time. With the Matthiensen's rule[20] it is possible to define a single relaxation time from which the mean-free path of the electrons on the Fermi surface can be calculated. In a thin film, additional collisions of the electrons with the film surfaces can occur. Fuchs[21] developed a theory to describe electrical conductivity in thin metal films, by assuming that the film is a plane parallel slab of bulk material. In addition, a real film consists of randomly oriented crystallites and the associated scattering at grain boundaries. Mayadas and Shatzkes[22] formulated a model which gave some qualitative predictions about this grain boundary scattering. In particular, this model relates the conductivity in a film to bulk conductivity through the diameter of an average grain and a reflection coefficient for electrons at grain boundaries. An additional modification of the resistivity must be introduced because voids can also modify the scattering relaxation time. Therefore, we estimated the conductivity of our films, starting from the bulk conductivity, modified by grain boundary scattering effects and the fraction of voids present. We find that the electron reflection coefficient is not constant, but depends on the conditions of film growth.

In this paper we describe the experimental details of sample preparation, including the parameters for film growth. The x-ray diffraction measurements and fluorescence analysis gave us details about the structure of these films, i.e., the expansion of the lattice, grain sizes, and densities. The optical measurements gave a measure of the fractions of voids, based on the free-electron model, effective media theory, and grain size in the films. Finally our electrical conductivity measurements were analyzed and interpreted on the basis of the now known grain size and fraction of voids.

II. FILM PREPARATION

The samples studied in this paper were prepared under ion bombardment in a dual ion-beam system. This technique, described elsewhere,[15] is based on the use of two broad ion-beam sources.[14] Figure 1 shows a schematic of the apparatus. The primary ion gun sputters the metal from a target and a secondary ion gun bombards the growing surface of the film. A crystal-quartz microbalance, positioned far enough away from the bombarding beams to avoid any interaction, measured the rate of the metal deposition. The ion current was measured by a Faraday detector placed on the rotating sample holder. With a background pressure of 10^{-9} Torr, sputtering was done from a 5-in. disk of silver with a purity of 99.99%. Pure argon gas was introduced to both the sputtering and bombarding ion guns at a partial pressure of 8×10^{-5} Torr. The ion energy in the primary ion gun was typically 700 eV with a ion-beam current of 10 mA, while the beam voltage of the secondary ion gun was 500 V. The

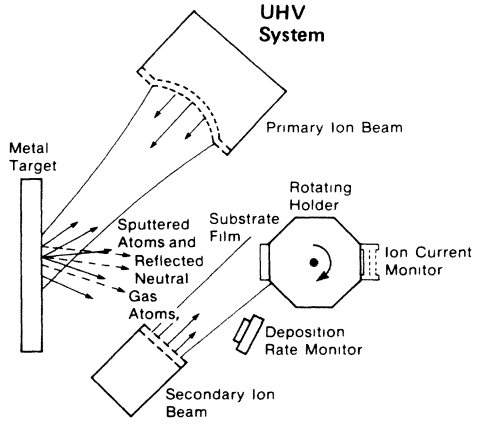

FIG. 1. Schematic of the dual ion beam apparatus.

conditions for film growth were set by adjusting the ion flux of the second gun between 1×10^{-7} and 1×10^{-8} A/cm^{-2}. The normalized energy E_n is defined as the ion energy per arriving metal atom at the substrate, i.e., the energy brought to the film by impinging Ar^+ ions divided by the number of arriving silver atoms. In the absence of ion bombardment the deposition rate was 0.25 Å/sec for all samples. Also all the depositions were performed at temperatures between 25 °C and 45 °C on substrates of amorphous fused silica carefully cleaned and outgassed under vacuum.

Samples were prepared at four different normalized energies: 20 eV, 42 eV, 100 eV, and 190 eV. The normalized energy for the 20 eV case was estimated from contributions of energetic neutral Ar gas atoms backscattered from the primary Ag target. This scattering process, extensively discussed in Refs. 23 and 24, originates from the primary ion flux being Auger neutralized at the target surface and quasielastically backreflected. Because of the various sources of error and the assumptions of the models,[25] this energy value of 20 eV may be only approximately correct. For the other samples the normalized energy was computed by adding the measured energies from the ion bombardment to the estimated contribution from the energetic neutral gas.

As a comparison standard for these films grown under ion bombardment, a separate silver thin film was prepared by evaporating silver from a tungsten boat in a vacuum system at a pressure of 10^{-7} Torr, the temperature and the substrate being the same as for the other samples.

III. X-RAY DIFFRACTION MEASUREMENTS

The structures of the Ag films were analyzed by the x-ray diffraction (XRD) method using a vertical θ-2θ scanning Norelco diffractometer automated with an IBM Series/1 minicomputer.[26] Data analysis for texture, lattice expansion, strain and grain size were done mostly with the host IBM 3083 computer. Details about the XRD measurement and analysis have been reported elsewhere.[27] Briefly, the degree of preferred orientation was evaluated from values of the normalized intensities

I_{200}/I_{111}, where I_{200} and I_{111} are the integrated intensities of the (200) and (111) reflections, respectively. The expansion of the silver lattice was calculated from the lattice spacing derived from the (111) reflection. The strain component normal to the surface of the film e_n was calculated from the change in lattice spacing, i.e., $\Delta d/d_0=(d_{111}-d_0)/d_0$.[28] Here d_0 is the (111) lattice spacing of strain-free Ag powder. The corresponding surface component of the strain e_s was then calculated with the equation derived by Witt and Vook.[29] The average grain size D was estimated by using the Scherrer equation.[30]

Our values for I_{200}/I_{111}, d_{111}, and D, for both evaporated and ion-bombardment films, are listed in Table I. For comparison, data of the randomly oriented Ag powder are also given at the bottom of Table I. These results showed that Ar ion bombardment has a pronounced effect on the structure of films. In comparison to the evaporated film, ion bombardment films showed less [111] preferred orientation; experienced a lattice expansion normal to the film instead of a contraction, i.e., showed tensile rather than compressive surface strain, and had significantly smaller grain sizes. These structural parameters, except the preferred orientation which was thickness dependent, varied systematically with E_n: at first rapidly, then leveling off as E_n reached $\sim$40 eV/atom and beyond.

IV. X-RAY FLUORESCENCE ANALYSIS

The densities ρ (mass per unit volume) of the Ag films were determined by the x-ray fluorescence (XRF) method. A wavelength dispersive spectrometer with a LiF analyzing crystal, scintillation counter, and single channel analyzer was used to collect the fluorescent Ag $K\alpha$ x rays. Using pure bulk Ag as a reference standard, we determined the areal density σ (mass per unit area) of the film by the fundamental parameter method.[31] The density was then calculated from $\rho=\sigma/t$, where t is the thickness of the film obtained from the attenuated total reflection method.[32]

Densities of the evaporated and ion-bombardment films are listed in the fifth column of Table I with an estimated precision of ± 0.2 gm/cm^3. The evaporated film had the highest density. The ion-bombarded process caused a reduction in ρ. At $E_n=20$ eV/atom, the density decreased by about 10%. Doubling the energy to 42 eV/atom reduced ρ another 5%, and any further increase caused no significant changes in ρ.

V. OPTICAL DATA

A. Measurements and analysis of the optical constants

For the optical measurements silver films were deposited with thicknesses close to 500 Å and as such were at the optimal thickness to support surface plasmons. The optical constants were then calculated from these reflectivity curves by attenuated total reflection in the Kretschmann[32] configuration on the base of a glass prism.[19] A typical reflection curve and calculated curve are shown in Fig. 2. By varying the angle of incidence, laser optical waves in the forward direction at the base of a prism could be matched to the propagation vector for the surface plasmon waves. When this occurred, energy was transferred from the laser beam into the optical surface mode and a reflectivity minimum results. We believe that the good agreement indicates that the derived optical constants are fairly accurate. These calculated dielectric constants were determined at each wavelength by analyzing the curves with the Fresnel equations,[33,34] and approximate values were improved by a nonlinear least-squares procedure.[19,34,35] The results are given in Table II for each of the laser wavelengths used in our experiments.

The angular position of the reflectivity minimum, as well as its depth and width, depends on film thickness and the real and imaginary parts of the dielectric function.[35,36] The specific dependencies on the parameters are not obvious. For example, the angular position is sensitive mainly to ε_1 and the thickness when the films are thinner than optimal. The depth depends on thickness and ε_2 at large values. A narrow reflectivity minimum is the result of a small ratio of the imaginary part to the real part of the dielectric function. However, the width is really a function of ε_1 and t. The optimal thickness for any metal has been shown to occur when the internal losses from the imaginary part equals that from reflective losses.[37] For silver this is at a thickness of about 500 Å, but for other metals, e.g., aluminum, it is closer to 200 Å. Further, these metals have much broader curves because $\varepsilon_2/\varepsilon_1$ is larger and they are less sensitive to effects of film struc-

TABLE I. Structural parameters deduced by x-ray diffraction and x-ray fluorescence. All the data are reported as function of the normalized energy.

E_n (eV/at.)	I_{200}/I_{111}	d_{111} (Å)	D (Å)	Density (g/cm^3)	Relative density[a]	Ar (at. %)
Evap.	0.07	2.3581	341	10.45	0.995	0
20	0.18	2.3606	200	9.55	0.910	0.18
42	0.16	2.3655	175	9.15	0.871	0.50
100	0.14	2.3664	162	8.95	0.852	0.80
190	0.12	2.3664	156	9.20	0.876	1.00
Powder	0.49	2.3591		10.50	1.000	0

[a]Relative density is compared to the bulk density, 10.50 g/cm^3.

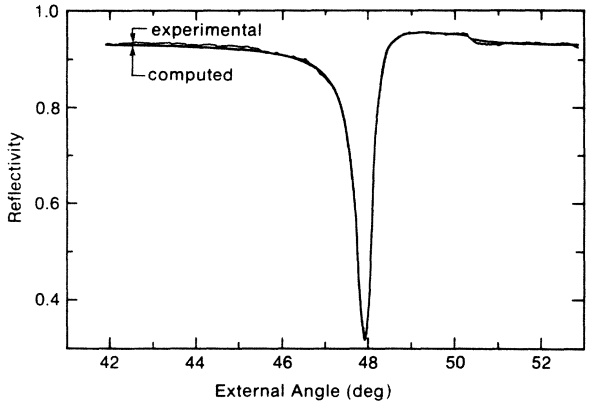

FIG. 2. Comparison between the experiment and the computed reflectivity vs angle at 6328 Å for a film grown at $E_n=20$ eV. The determined thickness and dielectric functions are given in Table II.

ture, including the surface.

B. Physics of the dielectric functions

The optical properties of a metal represent the response of the electrons to an applied electromagnetic field at optical frequency (10^{16} Hz) and can be expressed as a frequency-dependent complex dielectric function[33]

$$\tilde{\varepsilon}(\lambda)=\varepsilon_1(\lambda)+i\varepsilon_2(\lambda)\ , \tag{1}$$

where λ is the wavelength. We assume that our polycrystalline films averaged over the wavelength of light can be treated as isotropic (a good approximation for our films).

The dielectric function can be described by interband and intraband transitions of the free-electron gas depending on the frequency of the electromagnetic field. In silver these two components are quite distinct, and at energies lower than 2.8 eV, the optical properties are dominated by the intraband transitions.[16,33] In this spectral region the free-electron Drude model accurately describes the optical behavior, and the real and imaginary parts of the dielectric function can simply be written as

$$\varepsilon_1\cong\varepsilon_\infty-\frac{\omega_p^2}{\omega^2}\cong\varepsilon_\infty-\frac{\lambda^2}{\lambda_p^2} \tag{2}$$

and

$$\varepsilon_2\cong\frac{\omega_p^2}{\omega^3\tau}\cong\frac{\lambda^3}{\lambda_p^2\lambda_\tau}\ , \tag{3}$$

where λ is the wavelength of the light, and ω_p and λ_p are the plasma circular frequency and wavelength of the conduction electrons, respectively,

$$\omega_p=\left[\frac{4\pi Ne^2}{m}\right]^{1/2}\ . \tag{4}$$

ε_∞ represents the core polarizability and the contributions from interband transitions, τ the electron scattering time, and λ_τ the relaxation wavelength.

According to the free-electron Drude model, $-\varepsilon_1$ should be a linear function of λ^2. Figure 3 is a plot of our experimental results showing that $-\varepsilon_1$ does indeed vary linearly with λ^2. The different slopes depend on the conditions of film growth. In particular, the magnitude of ε_1 decreases as the energy delivered to the growing film increases. This can probably be interpreted as a change of a plasma frequency through its dependence on electron density which in turn is related to microstructure. The plasma wavelengths of our films were derived from Eq. (2). For each film the optical constants were determined at several spots on the film for several different wavelengths between 6328 and 4416 Å. Fortunately, only small variations were found. The results for λ_p at $E_n=0$ (0.1365 ± 0.0007 μm or 9.08 ± 0.05 eV) agreed very well with the values reported by Gugger *et al.*[19] (9.10 ± 0.02 and 9.14 ± 0.02 eV), and the value for ε_∞ close to 4 is also in agreement.

Of the factors which could change the electron density, a change in the lattice constant should be the most important; however, the increases found are not sufficient to account for the changes in the plasma wavelength. We believe this effect is possibly caused by the presence of voids.[18]

C. Effective-medium approach

The fraction of voids can be computed from the Bruggeman effective-medium approximation (EMA).[38] The measured effective-medium dielectric values are a function of the void fraction f_v

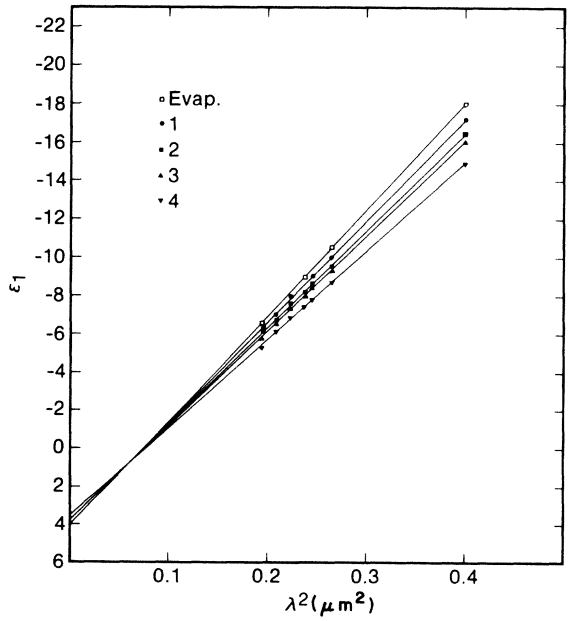

FIG. 3. Plot of $-\varepsilon_1$ vs λ^2 evaluated at the wavelengths reported in Table II for an evaporated film, and films experiencing ion bombardment at energies (1) 20 eV, (2) 42 eV, (3) 100 eV, (4) 190 eV.

TABLE II. Thicknesses, optical parameters, and void fractions at seven different wavelengths, and dc resistivities as functions of the normalized energy.

Normalized Energy (eV/Ag at.)	Wavelength λ (Å)	ε_{1EM}	ε_{2EM}	Thickness (Å)	Void fraction[a]	Resistance ($10^{-6}\omega$)
0	6328	−18.03	0.76	536		2.65
	5682	−13.50	0.60	542		
	5309	−11.20	0.53	545		
	5145	−10.34	0.47	536		
	4880	−8.81	0.39	528		
	4416	−6.40	0.35	531		
20	6328	−17.21	1.17	604	0.034	4.0
	5145	−10.03	0.68	602	0.026	
	4965	−9.11	0.64	598	0.030	
	4880	−8.81	0.64	586	0.019	
	4765	−8.04	0.56	594	0.034	
	4579	−7.06	0.53	597	0.039	
	4416	−6.16	0.48	601	0.043	
42	6328	−16.45	1.63	556	0.058	7.4
	5145	−9.51	0.93	559	0.054	
	4965	−8.64	0.86	554	0.057	
	4880	−8.15	0.76	556	0.059	
	4765	−7.60	0.70	556	0.062	
	4579	−6.63	0.68	558	0.069	
	4416	−5.82	0.69	559	0.069	
100	6328	−16.04	1.42	458	0.073	8.9
	5145	−9.36	0.78	423	0.063	
	4965	−8.41	0.73	424	0.070	
	4880	−7.99	0.71	424	0.069	
	4765	−7.35	0.69	425	0.078	
	4579	−6.51	0.62	424	0.078	
	4416	−5.76	0.57	424	0.074	
190	6328	−14.87	1.70	449	0.111	11.2
	5145	−8.41	0.92	409	0.098	
	4965	−7.81	0.94	403	0.104	
	4880	−7.43	0.90	403	0.102	
	4765	−6.87	0.88	403	0.108	
	4579	−6.03	0.80	409	0.111	
	4416	−5.28	0.75	403	0.110	

[a]Void fraction calculated from the dielectric functions and Eq. (5). See Sec. V D for a discussion and comparison of the void concentrations calculated from the measured dielectric functions and from the density measurements.

$$f_v\left[\frac{1-\tilde{\varepsilon}_{EM}}{1-2\tilde{\varepsilon}_{EM}}\right]=(f_v-1)\left[\frac{\tilde{\varepsilon}_m-\tilde{\varepsilon}_{EM}}{\tilde{\varepsilon}_m+2\tilde{\varepsilon}_{EM}}\right], \quad (5)$$

where the values of $\tilde{\varepsilon}_m$ are those for the bulk metal.[39] From the measurements at the seven different wavelengths, the fraction of voids for each film are listed in Table II. As expected, the fraction of voids increased with increasing energy. As anticipated, the plasma wavelength is a function of the fraction of voids, as shown in Fig. 4, and is an indication that the electron density is reduced by voids.

D. Void concentration estimated from density measurements

The presence of voids is also confirmed by simply relating the density of the films measured by x-ray fluorescence (see Table I) to the bulk density 10.50 g/cm.[2] The void fractions estimated from x-ray fluorescence data are larger than those estimated from the change in $\tilde{\varepsilon}$. This difference could be rationalized by assuming that a small fraction of voids were also present in the films used in Ref. 39 to determine the bulk optical constants. Extrapolating from our data the density of films used in Ref. 39

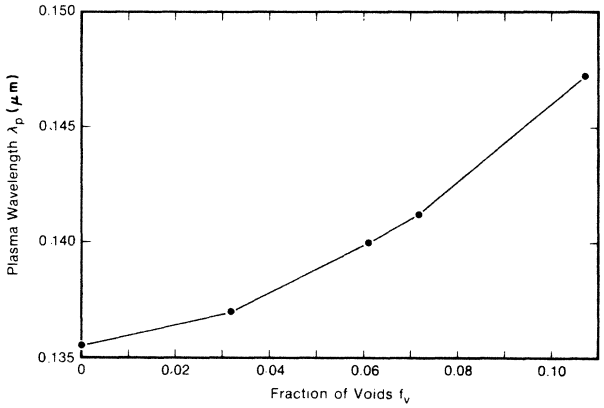

FIG. 4. Plasma wavelengths λ_p in microns vs the fraction of voids.

would be $\rho_B = 10.05$ g/cm^2, which implies a void fraction $f_v = 0.035$. This data regarding void fraction for films as reported in Ref. 39 is consistent with conclusions reached by Aspnes in Ref. 18.

E. Relaxation time analysis

It is more difficult to analyze the imaginary part of the dielectric function ε_2 because at least two mechanisms can contribute to an increase over the intrinsic bulk value. These are surface roughness and grain-size effects. Surface roughness acts mainly to increase the surface scattering at the film-air interface,[17,18] but in our experiment this problem could be eliminated. Scanning electron microscopy (SEM) measurements show that within 100 Å resolution our surfaces are very smooth. The effect of the grain size, however, could be more important. When the grain size becomes less than the bulk mean-free path for conduction electrons, the relaxation wavelength decreases and this may account for the observed increase in ε_2. The inverse in the relaxation wavelength (and the inverse relaxation time) can be derived from the slope of $\varepsilon_2\lambda$ versus λ^2 with the plasma wavelength determined from ε_1.

For the noble metals the scattering rate has the form[40]

$$\tau_{\text{eff}}^{-1} = \tau_{0F}^{-1} + \beta\omega^2 , \tag{6}$$

where τ_0 is the zero-frequency optical relaxation time, and β is a constant which depends on the material. Christy and co-workers[39,41,42] consider that this frequency dependence is caused by electron-electron scattering, but more recently Smith and Ehrenreich[43] have proposed that it follows from a more precise estimate of the electron-phonon interaction. Experimentally, Théye[17] showed that annealing thin gold films decreased the size of β. Nagel and Schnatterly[44] proposed an inhomogeneous medium model composed of crystalline grains and disordered intergranular material. We observed for all our films that the slopes, i.e., β, were all approximately the same yet our grain sizes varied considerably. Also the nonzero β values for single-crystal bulk samples[44] cannot be explained by grain size. Hence we cannot draw any conclusions about the relationship between β and grain size.

On the other hand, we found that τ_{0F} converged to approximately the same value, i.e., $\tau_{0F}^{-1} = 2\times10^{14}$ sec^{-1} for all the films grown under ion bombardment at various E_n. This behavior can be analyzed in terms of the influence of grain size on the intrinsic bulk relaxation time τ_0. In a thin metal, both volume and surface defects can affect the relaxation time. From the theory of anomalous skin effect it should be possible to separate the surface scattering contributions from those of volume. In this case the effective relaxation time at zero frequency can be written as

$$\tau_{0F}^{-1} = \tau_0^{-1} + \tau_S^{-1} + \tau_V^{-1} , \tag{7}$$

where τ_S and τ_V are the surface and bulk contributions, respectively. Now the surface contribution term depends mainly on two parameters, the film thickness and a surface scattering parameter.[18] When the film thickness is of the order, or greater than the electron mean free path, the influence of the surface is much reduced and will be neglected.

The contribution of volume scattering is mainly governed by imperfections, impurities, and grain size. The grain-size effect becomes most important when the particle diameter is comparable or less than the electron mean-free-path and the imperfections and impurities are mainly located around the surface of the grain. In this case, by assuming that the scattering length is equal to the average grain diameter D, the corresponding relaxation time becomes $\tau_G \cong 2v_F/D$, where v_F is the Fermi velocity, 1.38×10^8 cm/sec for silver.[45] Consequently, we simplified Eq. (10) (Ref. 18) to

$$\tau_{0F}^{-1} \cong \tau_0^{-1} + 2v_F/D . \tag{8}$$

In Fig. 5 the values of τ_{0F}^{-1} obtained from our optical measurements are plotted and compared to those calculated.

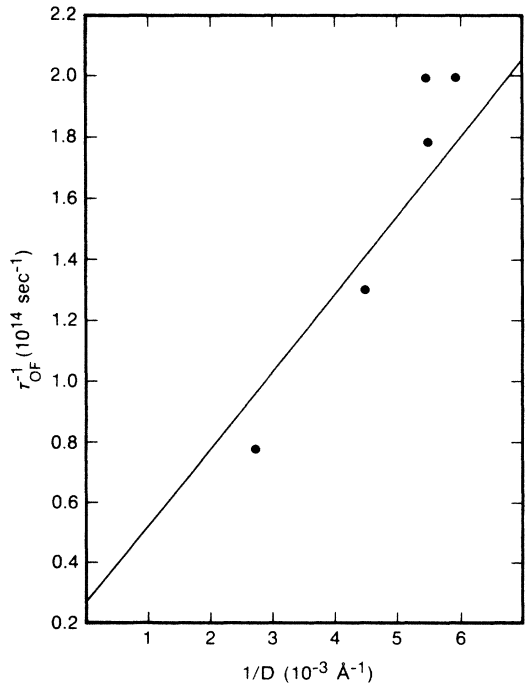

FIG. 5. Experimental and calculated values of τ_{0F}^{-1} vs $1/D$ (reciprocal grain size).

We used the average grain sizes listed in Table I (see the section x-ray diffraction measurements), the Fermi velocity given above, and $\tau_0^{-1}=0.26\times10^{14}$ sec^{-1}, which corresponds to a mean free path of 520 Å.[46] The correlation suggests that τ_{0F}^{-1} is mainly dominated by grain size, and other contributions, e.g., defects and vacancies, appear to be relatively unimportant. Therefore, we conclude that the voids should be due mainly to the intergrain spaces rather than voids within individual crystallites. This hypothesis seems to be also supported by detailed x-ray diffraction analysis that shows a nonrandom distribution of the dislocations[27] in our films.

VI. SPUTTERING GAS CONTENT

Films grown under conditions of ion bombardment often incorporate some of the sputtering gas. In the literature,[8–12,47,48] it is frequently reported that the amount of gas trapped in a film depends on the energy and flux of the bombarding ions.

The technique to measure the concentration, e.g., argon, described in detail in Ref. 49, is based on pulsed laser-induced flash evaporation of a known volume element of the thin film followed by quantitative analyses by mass spectrometer of the gases released. The measured equivalent number of argon atoms versus the normalized energies are reported in Table I and our results are in agreement with others[48] on different polycrystalline metals. The amount of argon did not exceed 1 at.%, which we believe to be too small to be considered as the origin of the lattice parameter deformation. To confirm this hypothesis, we report in Fig. 6 the lattice parameter enhancement versus the percent of Ar atoms. No consistent correlation exists.

This conclusion is also consistent with our electron spectroscopy for chemical analysis (ESCA) results which gave no evidence of a chemical shift due to Ar within the Ag crystallites even when the Ar content trapped in the film reached 1 at.%. Elemental Ar was also not seen by ESCA. A plausible explanation for these results is that the argon throughout the film is trapped between crystallites, e.g., at grain boundaries or voids but diffuses out of the upper most film layers so that ESCA would not see it. On the other hand, Citrin *et al.*[50] report significant chemical shifts in noble-gas ESCA spectra when a preexisting static metal surface is similarly ion bombarded. These results indicate that the gas trapped from ion bombardment during film growth ends up in different locations in a crystalline film structure than in the case resulting from similar ion bombardment of a preexisting static crystal lattice. It is well established that similar ion bombardment during film growth resulting in amorphous thin films leads to much larger percentages of the trapped bombarding gas. We will not consider gas content further in the subsequent analysis and discussion of the intrinsic properties of our Ag films.

If the grain boundary misfits are the origin of the stress, a correlation should exist between the total grain surface area, i.e., grain size, and the lattice parameters enhancement. Figure 7 shows that these two parameters are well correlated. As the particle size decreases, the lattice parameter increases. Similar particle sizes created under entirely different conditions, see Fig. 7, have similar lattice parameters. The normal and the surface stress, however, suggest that this effect is not isotropic.[27] An enhancement of the lattice parameters perpendicular to the surface should be compensated by a contraction in the plane. Two possible causes of this anisotropy suggest themselves: (1) the effect of void produce a nonisotropic deformation and (2) the stacking faults lie in preferential planes, very likely parallel to the surface. This hypothesis seems to be also supported by detailed x-ray-diffraction analysis that shows, in our films, a nonrandom distribution of the dislocation line.[27]

VII. FILM CONDUCTIVITY

It is well known that the resistivity of a thin metal film depends on thickness from the increased electron scattering at the surfaces compared to bulk and on the grain size due to electron scattering at grain boundaries. Fuchs,[21] using a Boltzman model, considered the probability for an

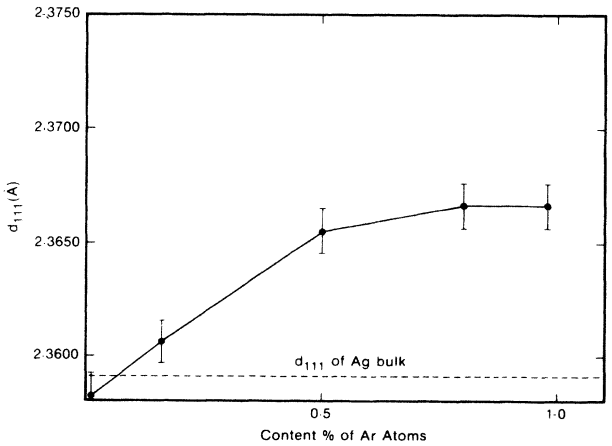

FIG. 6. Lattice spacing computed from the (111) x-ray diffraction peak vs the percent of Ar atoms trapped in the film.

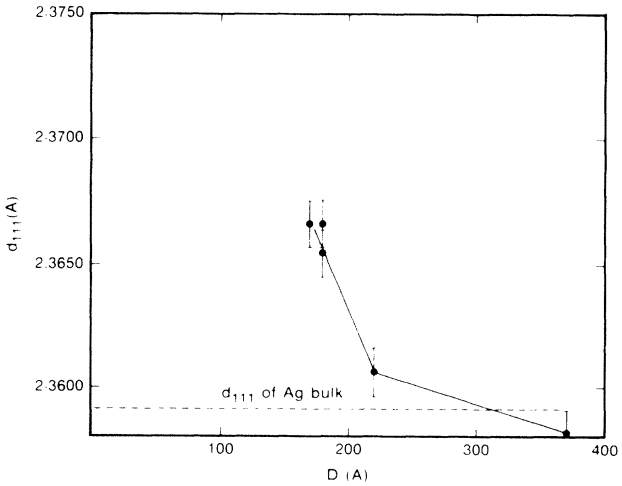

FIG. 7. Lattice spacing computed from the (111) x-ray diffraction peak vs the grain size.

electron to be reflected from a surface. His theory describes a free-electron gas in a thin metal film; however, for film thickness larger than the mean-free path λ_∞, i.e., $K=t/\lambda_\infty<1$, this contribution to resistivity becomes quite small.[20]

Effects from grain size, however, could be important because of the possible polycrystalline structure of some thin metal films, particularly, when the grain size is less than the electron mean-free path. Mayadas and Shatzkes[22] formulated a model which gives some qualitative predictions about grain-boundary scattering. The basic idea of this model assumes that the grain boundaries are all perpendicular with respect to the plane of the film and partially electron reflecting. The electron reflectivity R represents the probability for an electron at the Fermi surface to cross a potential barrier caused by lattice discontinuities. Its value is mainly determined by the shape of the Fermi surface and by the potential at the grain boundary[51] and these, in turn, are strongly dependent on the stress and mismatching among the grains.[52]

The ratio between the grain and the bulk conductivity is then given by

$$\frac{\sigma_G}{\sigma_B}=1-\tfrac{3}{2}+3\alpha^2-3\alpha^3\ln(1+\alpha^{-1}) , \tag{9}$$

where α is defined as

$$\alpha=\frac{\lambda_\infty}{D}\left[\frac{R}{R-1}\right] . \tag{10}$$

This one-dimensional model has been extended by Tellier and co-workers to three dimensions,[53,54] but this formulation contains, in our opinion, too many parameters to fit most experimental data unambiguously.[55]

The resistivity of our films was measured by using a standard dc four-probe procedure, normalizing the values to film thickness. In order to avoid heating of the sample, the measuring power was kept very low ($1-10\ \mu$W). Further, two voltage readings were taken at a reverse current to eliminate any spurious effects from thermal voltages. In Table II are reported the resistivity values for our films versus the normalized energy. The difference between the thermal evaporated sample and the highly ion-bombarded samples was about a factor of 4. Because thicknesses of the films were in a narrow range, between 480 and 560 Å, contributions dependent on thickness should be approximately the same for all of our films. Moreover, since $K\cong 1$ the surface scattering should be relatively unimportant. Therefore, it is likely that the observed changes in the electrical resistivity arise mainly from scattering at grain boundaries and from voids. On this basis we tentatively interpreted the experimental data using the grain-boundary model to obtain the grain conductivity and, subsequently, an effective-medium model to evaluate the effect of voids. Actually, the Mayadas-Shatzkes theory can only be correctly applied when the grain boundaries are perpendicular to the applied electric field. If we assume that the grain sizes we measured represent the isotropic average size for grains in three dimensions,[56] we can calculate the grain conductivity σ_G from Eq. (9) using a bulk silver conductivity (Ref. 57) $\sigma_B=0.629\times10^6\ \Omega^{-1}\,\mathrm{cm}^{-1}$.

The contribution of voids was evaluated by applying the Bruggeman effective-medium approximation[38] to the conductivity problem. Using the void fractions optically measured together with σ_G, and the bulk conductivity, the following expression gives the effective-medium conductivity σ_{EM}:

$$f_v\left[\frac{1-\sigma_{\mathrm{EM}}}{1-2\sigma_{\mathrm{EM}}}\right]=(f_v-1)\left[\frac{\sigma_G-\sigma_{\mathrm{EM}}}{\sigma_G+2\sigma_{\mathrm{EM}}}\right] . \tag{11}$$

In Fig. 8 we compare the calculated conductivities with the measured ones as a function of normalized energies for three different values of R. Our calculation gave a weak dependence of the resistivity on voids when their volume fraction ranged between 0 and 0.1, whereas the grain size seems to be a more important factor. In the limit of our assumptions, however, Fig. 8 suggests that the reflection coefficient R is different for each film and depends on the growing conditions or alternately the theory is inadequate. A possible explanation could come from the dependence of electron-reflection coefficient R on the shape of the Fermi surface and on the potential barrier at the grain boundaries, which in our case are expected to be different for each film as indicated by the structural changes, i.e., the lattice deformation, grain size, and voids.

VIII. CONCLUSIONS

From structural, optical, and electrical properties of silver films exposed to varying amounts of ion bombardment during the film growth, we have seen that the fraction of voids and the grain sizes in the metal film determine most of their nonbulklike behavior. Surface roughness and incorporated gases are unimportant in modifying the properties of our films as reported here. (The films

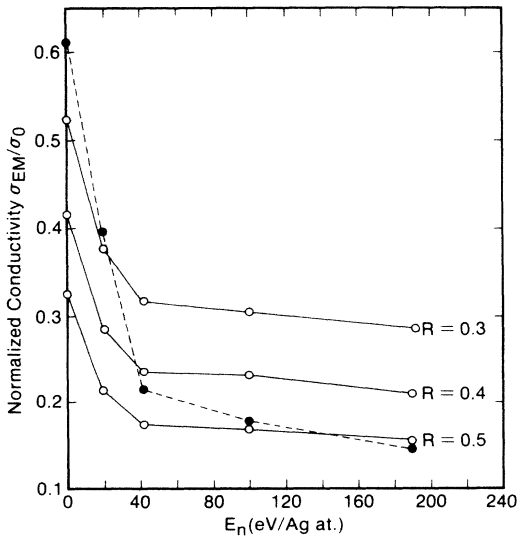

FIG. 8. Thin silver films normalized conductivities, $\sigma_{\mathrm{EM}}/\sigma_B$ computed for different values of R (solid lines) compared with the experimental normalized conductivities (dashed line).

were shown to be very smooth and the amount of entrapped gas was small.) Voids, through the change in electron density, were shown to modify the plasma frequency, and hence the real part of the optical dielectric function. The size of grains in the films, on the other hand, modified the relaxation times. The frequency dependency was essentially the same for all of our films, indicating that the electron-electron interactions and electron-phonon interactions were similar from film to film. (Ion bombardment did not seem to have any influence.) On the other hand, the observed lattice deformation, grain size, stress, and the measured quantity of voids were strongly dependent on the energy delivered to the growing film surface during film growth. In view of the fact that the sputtering gas trapped in the films did not correlate with the observed crystallographic anomalies, the most likely cause is, thought to be the lattice mismatching on the grain surfaces and the voids around the grains. Finally we showed that the electrical conductivity was influenced by both voids and grain size. However, to interpret completely the experimental data, it was necessary to assume a different electron reflectivity at the grain boundaries for films prepared under different conditions for each film. This hypothesis implies different potentials and different shapes of the Fermi surfaces as one approaches the surface of the individual crystallites, which is consistent with the observed dependence of the structural parameters on the growing conditions.

---

*Present address: Centro Informazioni Studi Esperienze, P.O. Box 12081, I-20100 Milan, Italy.

[1]J. M. E. Harper, J. J. Cuomo, and R. J. Gambino, *Ion Bombardment Modification of Surface: Fundamentals and Applications,* edited by O. Auciello and R. Kelly (Elsevier, Amsterdam, 1984), Chap. 4. See also references listed therein.

[2]J. J. Cuomo and R. J. Gambino, J. Vac. Sci. Technol. **14**, 152 (1977).

[3]R. Kelly, in *Proceedings of the Symposium on Sputtering,* edited by P. Varga *et al.* (Institut für allgemeine Physik, Technische Universität Wien, Austria, 1980), p. 390.

[4]H. F. Winters, D. L. Raimondi, and D. E. Horne, J. Appl. Phys. **40**, 2996 (1969).

[5]J. M. E. Harper, G. R. Proto, and P. D. Hoh, J. Vac. Sci. Technol. **18**, 156 (1981).

[6]D. W. Hoffman and M. R. Gaerttner, J. Vac. Sci. Technol. **17**, 425 (1980).

[7]R. Kelly, Nucl. Instrum Methods **182**, 351 (1981).

[8]P. Ziemann and E. Kay, J. Vac. Sci. Technol. A **1**, 512 (1983).

[9]E. Kay, J. Appl. Phys. **46**, 4006 (1975).

[10]E. Kay and G. Heim, J. Appl. Phys. **49**, 4862 (1978).

[11]P. Ziemann and E. Kay, J. Vac. Sci. Technol. **21**, 828 (1982).

[12]H. F. Winters and E. Kay, J. Appl. Phys. **38**, 3928 (1967).

[13]H. R. Kaufman, U.S. NASA Technical No. Note TND-585, 1961 (unpublished).

[14]H. R. Kaufman, in *Advanced in Electronics,* edited by L. Marton (Academic, New York, 1974), Vol. 36, p. 265.

[15]J. M. E. Harper, J. J. Cuomo, and H. T. G. Hentzell, Appl. Phys. Lett. **43**, 547 (1983).

[16]J. H. Weaver, C. Krafka, D. W. Lynch, and E. E. Koch, *Optical Properties of Metal—Part II* (Fachinformationszentrum Energie-Physik-Mathematik GmbH, Karlsruhe, Germany, 1981.

[17]M. L. Théye, Phys. Rev. B **2**, 3060 (1970); **18**, 2897 (1978).

[18]D. E. Aspnes, E. Kinsbron, and D. D. Bacon, Phys. Rev. B **21**, 3290 (1980).

[19]H. Gugger, M. Jurich, J. D. Swalen, and A. J. Sievers, Phys. Rev. B **30**, 4189 (1984).

[20]T. J. Coutts, *Electrical Conduction in Thin Metal Films* (Elsevier, Amsterdam, 1974).

[21]K. Fuchs, Proc. Cambridge Philos. Soc. **34**, 100 (1938).

[22]A. F. Mayadas and M. Shatzkes, Phys. Rev. B **1**, 1382 (1970).

[23]W. Heiland and E. Taglauer, Nucl. Instrum. Methods **132**, 535 (1976).

[24]S. H. Overbury, Surf. Sci. **112**, 23 (1981).

[25]J. Bottiger, J. A. Davies, P. Sigmund, and K. B. Winterbon, Radiat. Eff. **11**, 69 (1971).

[26]W. Parrish, G. Layers, and T. C. Huang, Adv. X-Ray Anal. **23**, 313 (1980).

[27]T. C. Huang, G. Lim, F. Parmigiani, and E. Kay, J. Vac. Sci. Technol. (to be published).

[28]C. S. Barrett, in *Structure of Metals* (McGraw-Hill, New York, 1966), pp. 466—476.

[29]F. Witt and R. W. Vook, J. Appl. Phys. **39**, 2773 (1968).

[30]J. I. Langford and A. J. C. Wilson, J. Appl. Crystallogr. **11**, 102 (1978).

[31]T. C. Huang and W. Parrish, Adv. X-Ray Anal. **22**, 43 (1979).

[32]E. Kretschmann and H. Raether, Z. Naturforsch. **23**, 2735 (1968).

[33]M. Born and E. Wolf, *Principles of Optics* (Pergamon, Oxford, 1980).

[34]O. S. Heavens, *Optical Properties of Thin Solid Films* (Dover, New York, 1965).

[35]I. Pockrand, J. D. Swalen, J. G. Gordon, II, and M. R. Philpott, Surf. Sci. **74**, 237 (1978).

[36]J. D. Swalen, J. G. Gordon, II, M. R. Philpott, A. Brillante, I. Pockrand, and R. Santo, Am. J. Phys. **48**, 669 (1980).

[37]I. Pockrand, Surf. Sci. **72**, 577 (1978).

[38]D. A. G. Bruggeman, Ann. Phys. (Leipzig) **24**, 636 (1935). See also J. C. M. Garnett, Philos. Trans. R. Soc. London **203**, 385 (1904); **205**, 237 (1906).

[39]P. B. Johnson and R. W. Christy, Phys. Rev. B **12**, 4370 (1972).

[40]P. O. Nilsson, in *Solid State Physics,* edited by H. Ehrenreich, F. Seitz, and D. Turnbull (Academic, New York, 1974), Vol. 29, pp. 218—221.

[41]R. T. Beach and R. W. Christy, Phys. Rev. B **16**, 5277 (1977).

[42]G. R. Parkins, W. E. Lawrence, and R. W. Christy, Phys. Rev. B **23**, 6408 (1981).

[43]B. Smith and H. Ehrenreich, Phys. Rev. B **25**, 923 (1982).

[44]S. R. Nagel and S. E. Schnatterly, Phys. Rev. B **9**, 1299 (1974).

[45]C. Kittel, *Introduction to Solid State Physics* (Wiley, New York, 1968), p. 208.

[46]F. W. Reinhold and G. R. Stilwell, Phys. Rev. **88**, 418 (1952).

[47]E. V. Kornelsen, Can. J. Phys. **42**, 364 (1964).

[48]J. J. Cuomo, J. M. E. Harper, C. R. Guarnieri, D. S. Yee, L. J. Attanasio, J. Angilello, C. T. Wu, and R. H. Hammond, J. Vac. Sci. Technol. **20**, 349 (1982).

[49]H. F. Winter and E. Kay, J. Appl. Phys. **43**, 789 (1972).

[50]P. H. Citrin and D. R. Hamann, Phys. Rev. B **10**, 4948 (1974).

[51]J. M. Ziman, in *The Physics of Metal,* edited by J. M. Ziman

(Cambridge University Press, Cambridge, 1969), pp. 264–268.

[52]W. A. Harrison, *Electronic Structure and the Properties of Solids* (Freeman, San Francisco, 1980), pp. 373–379.

[53]C. R. Tellier and A. J. Tosser, Thin Solid Films **57**, 163 (1979).

[54]C. R. Pichard, C. R. Tellier, and A. J. Tosser, Phys. Status Solidi B **99**, 353 (1980).

[55]J. R. Sambles, Thin Solid Films **106**, 321 (1983).

[56]Transmission electron microscopy confirms that this assumption is correct.

[57]R. C. Weast, *Handbook of Chemistry and Physics,* 57th ed. (CRC, Cleveland, 1977), p. F-167-8.